

Investigation of heavy ion tracks in polymers by transmission electron microscopy

A. Adla¹, V. Buschmann¹, H. Fuess¹, C. Trautmann²

¹ TU Darmstadt, ² GSI Darmstadt

Bulk samples and thin sections of polyethylene terephthalate (PET) and polyimide (PI) were irradiated with Se and Pb ions of 11.4 MeV/u at the UNILAC. The creation of latent tracks and related structural changes were studied by means of transmission electron microscopy (TEM) using a 200 kV Philips CM200-UTW microscope (point resolution 0.17 nm). Due to relatively similar electron densities within organic polymers, staining helps to increase the imaging contrast and improve the radiation resistivity under the electron beam.

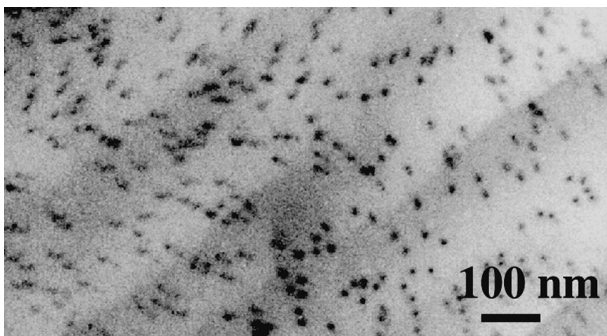


Fig. 1. TEM image of an originally 50 μm thick PET foil irradiated with Se-ions ($6 \times 10^{10} \text{ cm}^{-2}$, 900 MeV). The dark spots are the ion tracks decorated after irradiation by OsO_4 .

Typical stains such as OsO_4 or RuO_4 contain elements with high atomic number and diffuse preferably into the amorphous regions of the polymer thus enhancing the contrast of different structural regions. We investigated several sample preparation techniques, e.g. staining in vapor phase or aqueous solution, applied at different stages before and/or after ultra-microtomy and ion irradiation.

Fig. 1 shows the TEM micrograph of a PET sample irradiated as an initially 50-μm thick foil. Subsequently, the film was stained (aq. OsO_4 , 7 days) and cryo-sectioned perpendicular to the ion trajectories. The resulting ultrathin sections were stained again (2 h, OsO_4 vapor). The tracks are visible as dark spots indicating that the stain is preferentially accumulated in the amorphous track regions. The mean diameter is 12 ± 3 nm. The areal density is in good agreement with the ion fluence.

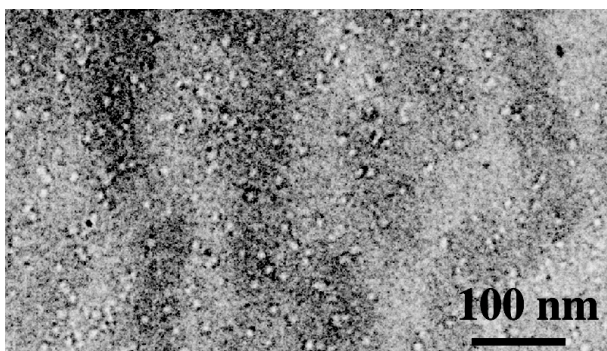


Fig. 2. TEM image of ultrathin section of PET, pre-stained (30 min, aqueous RuO_4) prior to irradiation with Pb-ions ($5 \times 10^{10} \text{ cm}^{-2}$, 2370 MeV).

The situation is quite different if pre-stained polymer samples are irradiated as thin sections (fig. 2). Tracks appear as light

features of reduced contrast with a mean diameter of 9 ± 1 nm. The stain and probably even the polymer material are expelled from the track region by sputtering and outgassing. Under a tilted angle, the number of tracks is twice as large as expected because we image two spots per track, namely the impact region on the front and back side of the sample. The track cylinders in the bulk are visible, but the contrast fades rapidly during observation.

Compared to PET, the electron-beam resistance of PI is better, allowing imaging at even higher magnifications. Fig. 3 presents a single track in a pre-stained (aq. RuO_4 , 2 h) and then irradiated 50-μm thick PI film. After ultramicrotomy, the thin section was stained again (OsO_4 vapor, 2 h). Note that in this case, tracks are imaged as bright regions although staining was performed after ion irradiation (cf. PET, Fig. 1). Since both, matrix and track regions, are amorphous, the selectivity of the post-staining process is apparently not high enough for preferential track decoration. In the matrix around the track, but not inside, the phase contrast of small crystalline areas of Ru or Os compounds can be recognized.

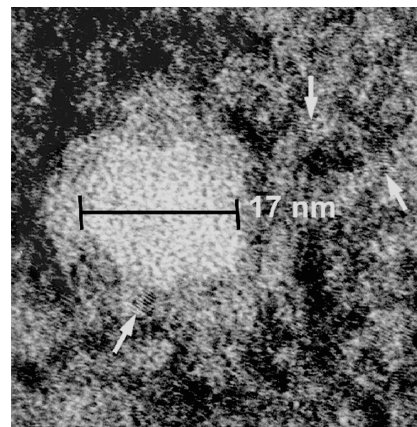


Fig. 3. High resolution TEM image of a single Pb-ion track in PI. The arrows indicate small crystalline areas in the track-surrounding matrix.

The track size observed here is in reasonable agreement however, slightly larger than diameters deduced earlier using other techniques such as small-angle x-ray scattering or IR-spectroscopy [1]. Also similar TEM studies on polyethylene [2] and on PI without staining [3] reported about 30% smaller track diameters. Finally, it should be mentioned that the precise determination of the track size in polymers using TEM is difficult due to the damage induced by the electron beam. The tracks may shrink or increase during imaging, making a direct comparison of different observations rather problematic.

- [1] C. Trautmann, K. Schwartz, T. Steckenreiter, Nucl. Instr. Meth. B156 (1999) 162.
- [2] J. Vetter, G. H. Michler, I. Naumann, Radiat. Eff. Def. Sol. 143 (1998) 273.
- [3] Y. Eyal, K. Gassan, Nucl. Instr. Meth. B156 (1999) 183.

Tracks of swift heavy ions in graphite studied by STM

J. Liu^{1,2}, R. Neumann¹, C. Trautmann¹, C. Müller¹

¹ GSI Darmstadt, ² Institute of Modern Physics, Lanzhou, China

Cleaved samples of highly oriented pyrolytic graphite (HOPG) were exposed to various beams of Ni, Zn, Xe, and U ions (11.4 MeV/u) with a fluence up to maximally 2×10^{12} ions/cm². To vary the kinetic energy and thereby the energy loss (dE/dx) of the ions, aluminum degraders of different thickness were placed in front of the crystals. The topography of the irradiated samples was investigated by scanning tunneling microscopy (STM) with constant current mode and with mechanically prepared Pt-Ir tips.

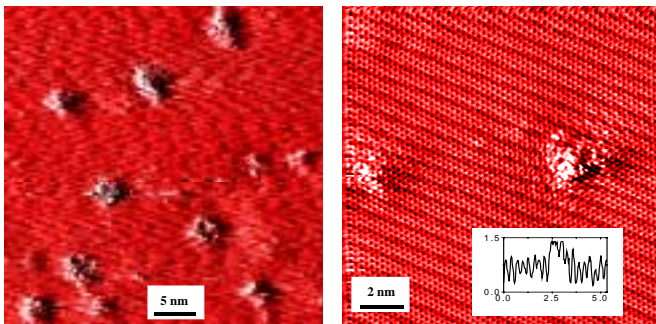


Fig. 1. STM images of original graphite surface bombarded under normal incidence with (left) 8×10^{11} U ions/cm² of 1.2 GeV and (right) 6×10^{11} Xe ions of 1.5 GeV. The inset shows a height profile across the hillock (scale in nm).

On the original surface, the tracks show extremely small hillock-like damage zones of mean diameters between 2 and 3.5 nm and heights of 0.3-0.9 nm (Fig. 1). Each protrusion is surrounded by the undisturbed crystal with lattice constant 0.246 nm. Fig. 2. presents the mean track diameter as a function of energy loss as calculated with the TRIM code.

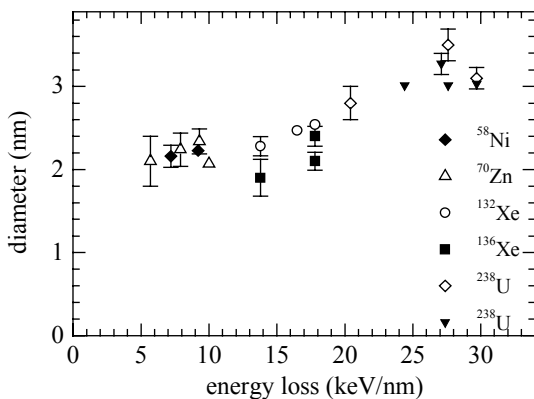


Fig. 2. Track diameter versus electronic energy loss. Tracks below 9 keV/nm are ascribed to nuclear collision processes.

In the dE/dx regime between 9-18 keV/nm, the areal density of observed protrusions is always smaller than the applied ion fluence. The creation yield as a function of the electronic

energy loss varies over several orders of magnitude (Fig. 3). A one-to-one relation was found only for ions above about 18 keV/nm. From a linear fit of the yield data for $9 \leq dE/dx \leq 18$ keV/nm, a threshold of 7.3 ± 1.5 keV/nm is deduced. Above this value, track formation on the crystal surface is unambiguously ascribed to electronic energy loss processes.

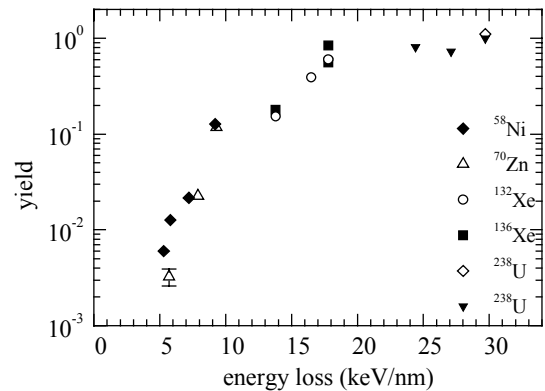


Fig. 3. Track creation yield defined as areal density of observed protrusions compared to the applied ion fluence on the original HOPG surface versus electronic energy loss.

We also recorded images from deeper bulk layers exposed by cleaving off thin slices from the crystal with an adhesive tape. On both adjacent lattice planes, hillocks are found, indicating that stress is relaxed towards the surface area around the impact site. The tracks are very similar to the features found on the original surface, however they are slightly (15-25%) reduced in size. Compared to the original surface, the probability for damage creation in the bulk is always significantly smaller. This phenomenon together with the dE/dx dependence of the yield observed on the surface can be understood, if we assume that the tracks consist of a discontinuous sequence of defect segments instead of a homogeneous damage cylinder.

Discussing track formation in graphite, the partly metallic character due to the lamellar structure has to be taken into account. The high thermal and electrical conductivity parallel to the layers allows efficient dissipation of the projectile energy radially from the ion path. Since graphite is a monoatomic crystal, we certainly have to consider that the disordering of the lattice is followed in time by a rapid recrystallisation occurring in particular in the bulk [1].

[1] L.T. Chadderton, D. Fink, Radiat. Eff. Def. Sol. 152 (2000) 87.

Charge collection with a Microbeam : Prospect for determination of ion track profile

T. Colladant^{1,2}, ¹GPS Université Paris 6 – 7 (France), ²CEA-DIF (France)
 O. Musseau, V. Ferlet-Cavrois, CEA-DIF (France)
 A. B. Campbell, NRL (USA)
 B. Fischer, M. Schlögl, GSI (Germany)

Introduction

Single event effects (SEE's) induced by heavy-ions from cosmic-rays are a major problem for the reliability of microelectronic devices in space environment. The energy deposited by a heavy-ion through the sensitive structure of a device produces, in a very short time, a dense concentration of electron-hole pairs along the ion trajectory. Generated carriers are collected by drift (if there is a local electric field) or by diffusion over hundreds of picoseconds. Previous works showed that differences in charge collection depend on the initial ion track structure [1][2].

Codes proposed by atomic physicists for ion tracks as TRKRAD [3] or TRIPOS [4] calculate a track profile which does not take into account the carrier thermalization and the recombination in the core of the track. For actual and future device generations, the knowledge of the ion track structure becomes necessary to correctly simulate the interaction within a device which has dimensions smaller than the ion track radius.

Test structures were fabricated in order to determine experimentally the effective size of an ion track and the carrier density profile [5][6]. They consist either of Schottky-barrier junctions or PN junctions on a silicon line.

Experiments

Following this way, Schottky-barrier junction microstrips are investigated here. They are made up of three lines (0.5 μm width with a 1.5 μm pitch) connected together. Schottky-barrier junctions were processed on a Silicon On Insulator (SOI) substrate to avoid long-distance charge collection, with a 0.6 μm thick silicon film (figure 1-a).

The devices were irradiated using the GSI scanning ion microprobe with 99.6 MeV carbon ions (LET=1.44 MeV.cm².mg⁻¹ [7]). The microbeam spot diameter was 0.5 μm . All the electrodes were grounded during experiments including the metal lines via the charge preamplifier input impedance. When an ion strikes one of the lines, a charge is generated and detected by the amplifier chain. This collected charge and the coordinate of the ion strike are recorded by a multiparameter data taking system. The resulting charge collection image is shown (figure 1-b) after correction by an offset angle with respect to X and Y axis.

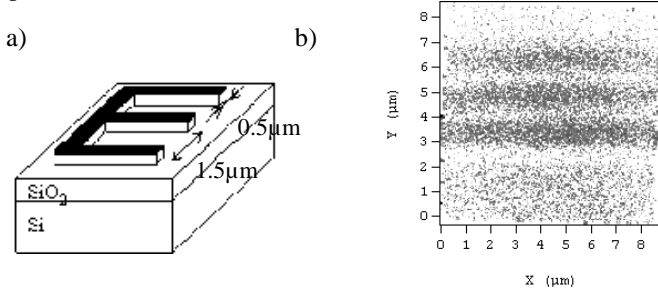


Figure 1: (a) Cross section of the tested devices, (b) charge collection image from experimental data (the dark area correspond to large collected charges).

Charges are collected in the Schottky-barrier junctions by drift due to the local electric field in the depletion region (thickness of about 0.13 μm) and by funneling effect. Charges collected from ion strikes outside the lines could be due to a capacitive coupling between silicon film and the substrate, and to a local electric field in the silicon near the oxide interface caused by trapped charge in the oxide from previous scanning.

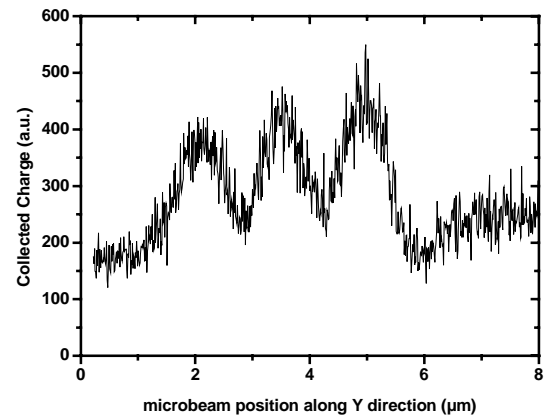


Figure 2: collected charge profile along Y direction.

An experimental charge collection profile is extracted from the charge collection image by integrating data over the X direction (figure 2).

Note that the ratio between the charge collected when the ion strikes a line and the bare SOI substrate is only 2. Thus, only the microbeam allows to extract the charge collected by lines, by rejecting the SOI substrate signal thanks to its small probing surface. This would indeed not be possible with a standard heavy ion beam.

Conclusion

The ion microbeam is the only technique which allows us to spatially measure the collected charge on Schottky-barrier junctions with a good signal to noise ratio.

With a complete understanding of the charge collection mechanisms by drift-diffusion simulations, it may be possible to correlate the charge collection on the strip with the ion track profile.

References

- [1] H. Dussault et al., IEEE Trans. Nucl. Sci. NS-40, pp. 1926-1933 (1993)
- [2] W. J. Stapor et al., IEEE Trans. Nucl. Sci. NS-35, 1585-1590 (1988).
- [3] W. J. Stapor et al., J. Appl. Phys. 64, pp. 4430-4434 (1988).
- [4] R. C. Martin et al., Physica Status Solidi A 104, pp. 743-754 (1987).
- [5] J. W. Howard et al., IEEE Trans. Nucl. Sci. NS-41, pp. 2077-2084 (1994).
- [6] O. Musseau et al., IEEE Trans. Nucl. Sci. NS-45, pp. 2563-2570 (1998).
- [7] J.F. Ziegler et al, SRIM-2000.10, 1999 IBM Co.

Influence of Heavy Ion Induced Columnar Defects on the Vortex Dynamics of High-Temperature Superconductors

M. Basset¹, G. Jakob¹, G. Wirth², B. E. Fischer², P. Voss-de Haan¹, E. Jäger², and H. Adrian¹

¹ Institut für Physik, Johannes Gutenberg-Universität, D-55099 Mainz

² Gesellschaft für Schwerionenforschung, D-64291 Darmstadt

The investigation of vortex dynamics in high-temperature superconductors (HTSC) is always related to the question of defects. In the presence of random disorder the long range order of the magnetic flux line lattice is destroyed and a vortex glass (VG) phase [1] is established below a characteristic glass temperature T_G . In the presence of heavy ion induced columnar defects this correlated disorder leads to a transition from vortex liquid to a Bose-glass (BG) phase [2]. In both cases this transition can be described with the appropriate scaling theory. For the BG case the scaling relation between current density J and electric field E is described by

$$\ell_{\perp}^{z'-1} E \approx \varepsilon_{\pm} (\ell_{\parallel} \ell_{\perp} J) \quad (1)$$

with length scales ℓ_{\parallel} and ℓ_{\perp} parallel and perpendicular to the columnar defects that diverge as

$$\ell_{\perp} \propto (T_{BG} - T)^{\nu_{\perp}} \quad (2)$$

where ν_{\perp} and z' are the static and dynamic exponents.

We performed electrical transport measurements on epitaxial $\text{YBa}_2\text{Cu}_3\text{O}_{7-x}$ thin films. Due to their extremely long measurement bridges $l=10.9$ cm that were patterned photolithographically we were able to measure current-voltage characteristics with an electric field resolution of 10^{-8} V/m and recent results have shown that the dynamic exponent of the VG transition in unirradiated thin films strongly depends on the experimentally accessible range of the electric field [3] which is in contrast to the theory. In order to study the dependence of the critical exponents from the electric field range we have irradiated the samples subsequently with 0.752 GeV ^{209}Bi , $B_0 = 0.6$ T and 0.749 GeV ^{208}Pb , $B_0 = 1.0$ T, $\Sigma B_0 = 1.6$ T. For this energy both ions have nearly the same electronic energy loss S_e which is responsible for the creation of columnar defects. We performed the same measurements as for the unirradiated case and the obtained data can be scaled well within the framework of the BG model for different magnetic fields. In accordance with the unirradiated case we could show that the dynamic critical exponent z' in the BG case also depends strongly on the electrical field range.

Another consequence of the irradiation is that the number of pinning centers for the vortex system is increased and the glass temperature T_G is shifted. Figure 1 shows the (H, T_G) -irreversibility line for the different irradiation doses and the unirradiated case respectively. For a magnetic field $\mu_0 H = 1$ T the glass temperature is increased linearly with the irradiation dose as shown in the insert of Fig. 1.

We additionally take advantage of the different vortex dynamics in irradiated and unirradiated parts of HTSC thin films to study the effects at the interfaces between these regions. Different methods can be applied to prepare such a

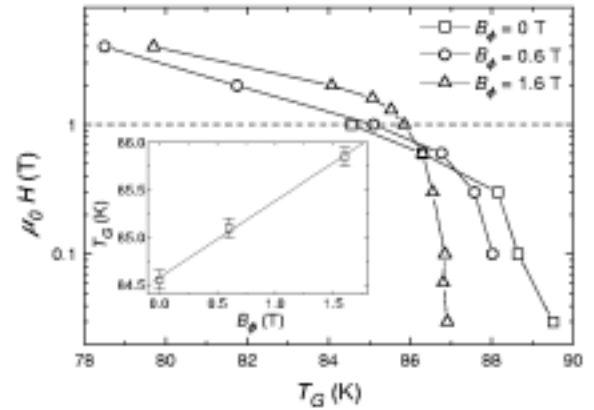


Figure 1: Irreversibility line before and after heavy ion irradiation. For $B_0 = 0$ T the glass temperature is determined using VG scaling, whereas the BG model is used for the irradiated sample. The number of coherent pinning centers is increased and the (H, T_G) -line is shifted. The insert shows the linear dependence between B_0 and T_G for a magnetic field $\mu_0 H = 1$ T.

Bose-glass contact. In a first experiment we created a periodic array of strong and weak pinning channels using metal masks or the GSI-microprobe. These channels of width between $10 \mu\text{m}$ and $800 \mu\text{m}$ lead to a guided vortex motion (GVM) that can be detected by measuring in a Hall geometry [4]. We have shown that the characteristic fields and temperatures of this GVM are correlated to the BG phase. The second experiment currently is focussed on the electric field profile of a BG contact. Several equidistant ($20 \mu\text{m}$) voltage probes allow to measure the electric field across the interface between irradiated and unirradiated regions. The measured electric field profile of the weak pinning channel contains information about the characteristic length scales of the interaction between pinned and free vortices.

Thus vortex dynamics at the interface of a BG contact is a new field of investigation to study vortex-vortex interactions in HTSC thin films. Two experimental techniques are necessary to obtain more information: nanolithography and the GSI-microprobe in order to create irradiation patterns on a microscopic scale. This will be realized within the framework of the collaboration.

References

- [1] D. S. Fisher *et al.*, Phys. Rev. B **43**, 130 (1991).
- [2] D. R. Nelson *et al.*, Phys. Rev. B **48**, 13060 (1993).
- [3] P. Voss-de Haan *et al.*, Phys. Rev. B **60**, 12443, (1999).
- [4] M. Basset *et al.*, submitted to Phys. Rev. B

On the low temperature mixing processes in metal/ceramic interfaces

R. Nagel and A.G. Balogh

Institute for Materials Science, Darmstadt University of Technology, Petersenstrasse 43, 63741 Darmstadt

Heavy ions in materials science can be used for many applications concerning changes in composition, structure and physical properties. The modification of interfaces in bi-layer samples is frequently performed by ion beam mixing experiments [1-4]. However, the mixing behaviour of the components is much more complicated than in the earlier studied metal/metal systems, because of the more complex structure of the ceramic materials.

Samples with different composition (Fe, Cu, Ni, Pt, Zr, Ti and TiO₂ on Al₂O₃, SiO₂, MgO and SiC-substrates) were prepared by molecular-beam-epitaxy. The samples were irradiated at the GSI 300kV implantation facility with 150 keV Ar⁺ ions at different temperatures. Rutherford backscattering spectroscopy (RBS) was used to obtain the element depth profiles. The surface topography and the surface roughness was studied with a high resolution scanning electron microscope (Philips XL 30 FEG) and with atomic force microscopy (AFM).

The RBS spectra were converted to depth profiles by using the computer code *ndf* [5]. The width (σ_I) and the position of the interface was calculated using an error function. The measured and calculated mixing rates are shown in figure 1. In many systems (Cu/Al₂O₃, Cu/SiC, Fe/Al₂O₃, Fe/SiO₂, Fe/SiC,

Ni/Al₂O₃, Ni/SiO₂, Ni/MgO, Ni/SiC, Pt/Al₂O₃, Pt/SiC, Zr/Al₂O₃, Zr/SiO₂, Ti/SiO₂ and TiO₂/SiO₂) the low temperature data can be interpreted using the binary collision model (BCS) [6] alone (fitted line in the upper part of fig.1). For the systems Cu/Al₂O₃, Fe/MgO, Cu/SiO₂, Ni/SiO₂, Pt/SiO₂ and Cu/MgO the measured values exceed the predictions of the BCS model. Therefore the model was expanded following the approach of Refs. [7-8]. The ion beam mixing rates will be enhanced in this compound model by a factor, which is the ratio between the atomic densities of the mixing species. Using the expanded c-BCS model all data points could be fitted correctly as it is shown at the lower part of fig.1. However, the difference between the predictions of the BCS model and the measured values can be also explained assuming the formation of local thermal spikes. After Cheng [9] the space filling character of the collision cascade, as primary condition for the formation of thermal spikes, is only possible, if the energy transferred to the recoils (E_R) is lower than the spike initiation threshold energy $E_{TS}=0.039eV*Z^{2.23}$, but higher than the displacement energy (E_d). Taking the Ni/Al₂O₃ system as an example, this means, that the formation of local thermal spikes will be allowed, if the recoil energy falls between 16 and 28 eV.

References

- [1] K.Neubeck, C.E.Lefaucheur, H.Hahn, A.G.Balogh, H.Baumann, K.Bethge, D.M.Rück, NIM B, 106 (1995) 58
- [2] K.Neubeck, H.Hahn, A.G.Balogh, R.Hausner, H.Baumann, K.Bethge, D.M.Rück, NIM B, 113 (1996) 186
- [3] R.Nagel, H.Hahn, A.G.Balogh, NIM B, 148 (1999) 930
- [4] R.Nagel, A.G.Balogh, NIM B, 156 (1999) 135
- [5] N.P.Barradas, C.Jeynes, R.P.Webb, Appl. Phys. Lett., 71 (1997) 291
- [6] P.Sigmund, A.Gras-Marti, Nucl.Instr.Meth., 25 (1981) 182
- [7] J.Desimoni, A.Traverse, Phys.Rev.B, 48 (1993) 13266
- [8] S.Dhar, Y.N.Mohapatra, V.N.Kulkarni, Phys.Rev.B, 54 (1996) 5769
- [9] Y.T.Cheng, Mat.Sci.Rep., 5 (1990) 45

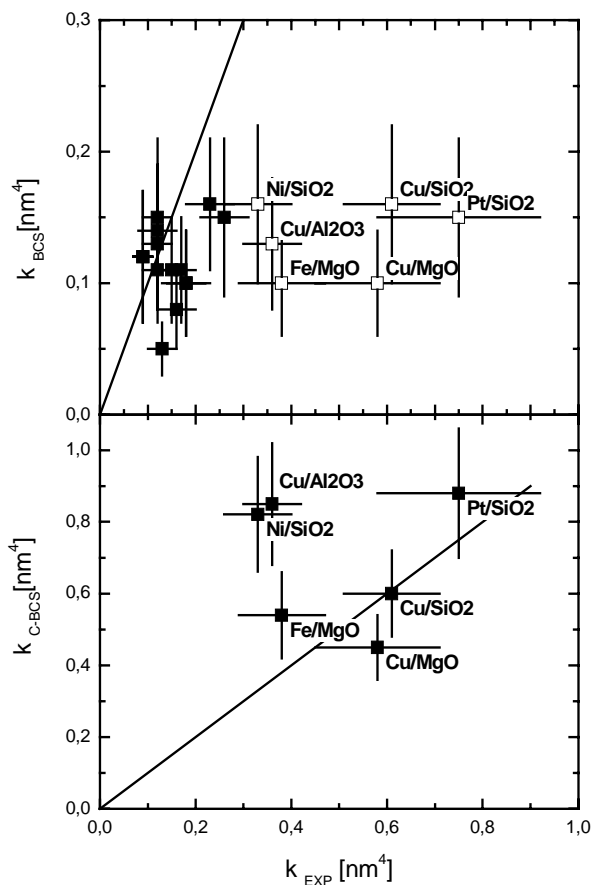


Fig. 1.: Measured and calculated mixing rates for different systems. At the top: fitted by the BCS model, at the bottom: fitted by the compound-BCS model.

Conducting ion tracks in diamond-like carbon films

A. Weidinger¹, C. Trautmann², J. Krauser¹, V. Hoffmann¹, N. Stolterfoht¹, H. Hofsäß³, B. Schultrich⁴, H. Sturm⁵,
¹HMI Berlin, ²GSI Darmstadt, ³Univ. Göttingen, ⁴FhG Dresden, ⁵BAM Berlin

The formation of ion tracks in diamond-like carbon (DLC) films on conducting Si substrates is studied. The films were produced by either conventional ion beam techniques (Univ. Göttingen) or by plasma deposition with magnetic filtering (filtered arc method, FhG Dresden). In both cases, the ions were implanted into the growing film with an energy in the order of 100 eV, thus creating by "subplantation" the conditions required for diamond formation. Such films are amorphous, contain 70-80% sp³ bonds, and in the present case, have a thickness 40 and 100 nm, respectively.

The ion irradiation of the DLC films was performed at the UNILAC with Uranium projectiles of ~1 GeV (moderated down from 2.7 GeV by Al foils). Due to the high energy deposition of the ions along their trajectories, the material is transformed from insulating diamond-like to conducting graphite-like carbon leading to thin electrically conducting channels embedded in an insulating matrix [1]. The properties of these channels were studied by means of scanning probe microscopy (AFM) using a conducting tip.

Figure 1 shows a three-dimensional AFM image of the surface topography of the irradiated DLC film. Hillocks with a few nm in height and ~20 nm in diameter are seen at the ion impact sites. The number of hillocks corresponds to the applied ion fluence.

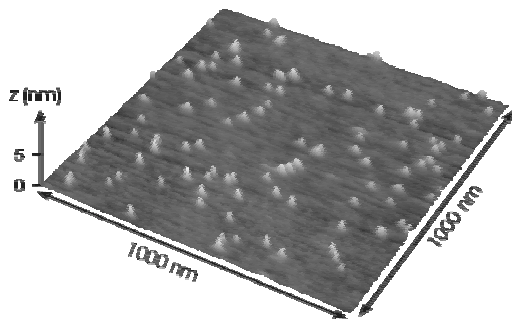


Fig.1 Topographical AFM image of a DLC film (FhG Dresden, 40 nm thick) irradiated with 10¹⁰ uranium ions per cm² of 1 GeV. The hillocks are due to the outflow of material at the ion impact site.

Figure 2 shows a three-dimensional plot of the current flowing between the AFM tip and the Si substrate through the DLC film. Each of the spikes corresponds to an ion track. Outside of the tracks the current is practically zero. Note, the current image originates from a different sample than the topographic image in figure 1.

The current between the substrate and the AFM tip as a function of voltage is presented in figure 3 for a spot on an ion-track and a spot outside of the track, indicating the overall noise level of the non-irradiated sample.

Assuming a track cross section of 100 nm², the measured current at 5 V gives a current density of 10⁴ A/cm² and a electrical resistivity of $\rho = 50 \Omega\text{cm}$. The conductance of the tracks is four orders of magnitude smaller than that of

crystalline graphite, thus a very defective graphite filament is formed.

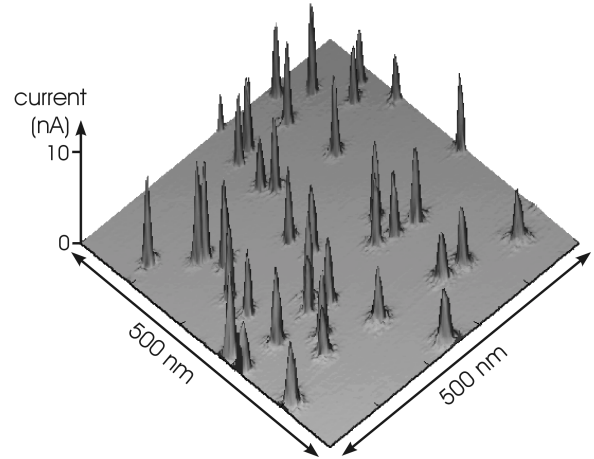


Fig.2 Current image of a DLC film (Univ. Göttingen, 100 nm thick) identically irradiated as sample of fig. 1. The current measurements were performed with a conducting AFM tip.

The general perspective of this kind of research is seen in the possibility to create nanostructures of materials which have properties distinctly different from the surrounding. In the present case, thin conducting filaments of graphite are embedded in an insulating diamond-like matrix. Such filaments may be useful in future mechanical or electrical nano-devices. A more immediate application is seen in the use of these tracks as electron field emitters in displays or other vacuum electronic devices (to replace hot filaments).

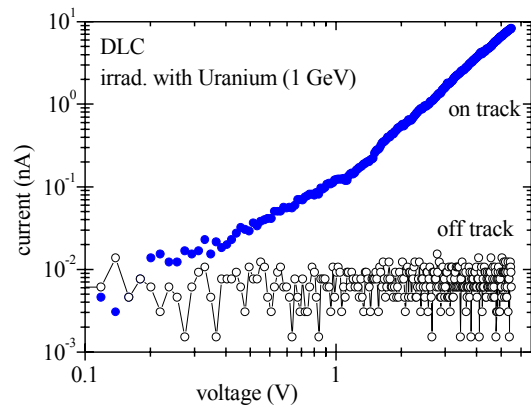


Fig.3 Current/voltage curve for a single ion track (AFM tip on top of a track). For comparison, the corresponding curve for the off track position is shown. DLC film from Univ. Göttingen, 100 nm thick.

[1] M. Waiblinger, Ch. Sommerhalter, B. Pietzak, J. Krauser, B. Mertesacker, M.Ch. Lux-Steiner, S. Klaumünzer, A. Weidinger, C. Ronning, H. Hofsäß, *Appl. Phys.* **A69** (1999) 239.

Visualization of latent alpha-recoil tracks in dark mica by scanning force microscopy

¹Glasmacher, U.A., ²von Grabczewski, N., ²Heiß, M., ²Neumann, R. & ¹Wagner, G.A.

¹Forschungsstelle Archäometrie der Heidelberger Akademie der Wissenschaften am Max-Planck-Institut für Kernphysik, P.O. Box 103980, D-69029 Heidelberg, Germany, ua.glasmacher@mpi-hd.mpg.de;

²Gesellschaft für Schwerionenforschung (GSI), Planckstrasse 1, D-64291 Darmstadt, Germany,

As a natural mineral, dark mica contains α -emitters such as uranium and thorium. During their α -decay, part of the recoil energy is transferred to the daughter nuclei. These interact with the surrounding crystal lattice where they create 'nest-shaped' radiation damage, so-called alpha-recoil tracks (ART). If the volume density of such ART as well as the concentration of the α -emitters is known, one can evaluate the age of the sample [1]. For the registration of the ART volume density via optical phase contrast microscopy, the tracks have to be etched to a certain size. The etch pits are triangular in shape. If the track density is too high, the pits cannot be enlarged above the optical resolution of the microscope without overlapping. Therefore, up to now ART dating is restricted to dark micas of ages not exceeding 10^6 a.

To overcome this age limit, scanning force microscopy (SFM) was applied to visualize latent ART. Natural biotite from the Altai Mountains, China, was used to test whether SFM is able to image latent ART and, thus, suitable for the dating of older dark micas. Scanning the surface of freshly cleaved biotite did not reveal any tracks. Subsequently, this surface was kept in ambient conditions over a certain time period. Within several hours, small hillocks developed with an initial size as expected for latent ART in dark mica (see Figure 1).

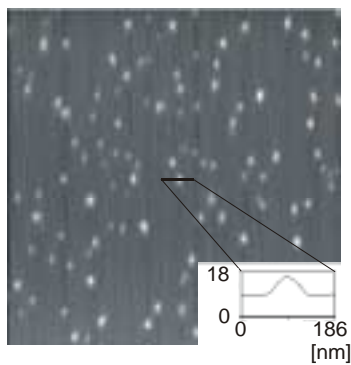


Figure 1: Topographic SFM image ($2.4 \mu\text{m} \times 2.5 \mu\text{m}$) of a biotite cleavage plane kept in ambient conditions for several hours. Light areas represent hillocks. Both inset scales are in nm.

Diameter and topographic height increased with time, reaching a saturation limit several days after cleavage. The damaged material has a lower hardness than the intact surroundings. The areal density of tracks is similar to that of ART revealed by etching and phase contrast microscopy. After very short etching of the surface, the SFM image indicated triangular etch pits rather than the previously occurring hillocks (see Figure 2). These pits look similar to the etched ART in lower resolution (phase contrast microscopy).

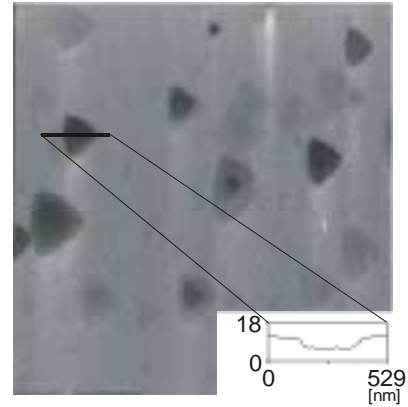


Figure 2: Topographic SFM micrograph ($2.9 \mu\text{m} \times 3.0 \mu\text{m}$) of biotite after short etching, showing triangular etch pits.

Heating the biotite at $500 \text{ }^\circ\text{C}$ for 30 min annealed the latent ART. The annealed material was irradiated at the UNILAC of GSI with $^{136}\text{Xe}^{18+}$ and $^{238}\text{U}^{28+}$ ions at $E_{\text{kin}} = 11.4 \text{ MeV/u}$ and fluences of 5×10^{10} and 1×10^{10} ions/ cm^2 , respectively. Scanning these samples revealed hillocks. Etching develops the artificially created hillocks into circular rather than triangular etch pits (see Fig. 3), in contrast to the behaviour of the hillocks displayed in Fig. 1, which are attributed to alpha-recoil tracks.

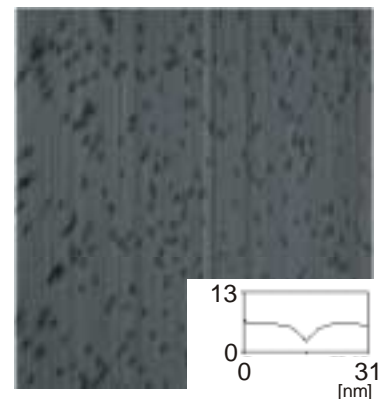


Figure 3: Topographic SFM image of irradiated ($^{136}\text{Xe}^{18+}$, fluence: 5×10^{10} ions/ cm^2) biotite after short etching (size: $830 \text{ nm} \times 860 \text{ nm}$).

In conclusion, visualization of latent ART by SFM enables us to reveal track densities beyond 10^8 cm^{-2} and thus extend the new ART dating technique to an age range $> 10^6$ a.

- [1] Gögen, K., Wagner, G.A., 2000. Alpha-recoil track dating of Quaternary volcanics. *Chemical Geology* 166, 127-137.

Investigation of X-ray and ion irradiated DNA using scanning force microscopy

M. Hei, G. Taucher-Scholz, N. von Grabczewski, R. Neumann
GSI Darmstadt

It is well known that the biological effectiveness for cell inactivation of radiation with high linear energy transfer (LET) around 100 keV/ μm is higher than the one of low-LET radiation [1]. The reason for that may rely on the fact that double-strand breaks (DSB) of DNA-molecules induced by high-LET-radiation are repaired less efficiently than those, which are induced by low-LET-radiation [2]. This could be caused by a different spatial distribution of DSB, in connection with the inhomogeneous distribution of dose. To verify this hypothesis it is desirable to directly investigate the condition of DNA after irradiation.

In our work we did these investigations on plasmid DNA irradiated with X-rays and ions using scanning force microscopy (SFM). Therefore we developed a preparation method which allowed us to determine the fractions of the different plasmid conformations and additionally measure the length of DNA fragments in the pictures produced by the SFM (see Figure 1)

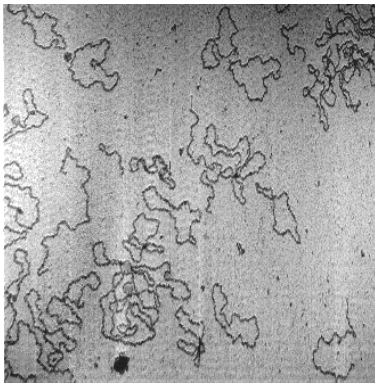


Figure 1: Typical SFM picture of DNA
(size: 3 μm x 3 μm)

Using this preparation method we studied ΦX174 plasmid DNA that was irradiated in 20 mM HEPES buffer in a supercoiled compact conformation with different doses of X-rays and Zn-ions.

As a result we obtained for every sample the fraction of each different plasmid conformation (see Figure 2) and the fragment distributions. From this we were in addition able to determine the mean fragment-lengths as well as the number of DSB per broken plasmid (see Figure 3).

In figure 2 the difference between high- and low-LET radiation in the production of DNA-DSB can be seen. For X-rays the linearised fraction increases

quadratically with dose while for ions in the lower dose region this fraction increases linearly.

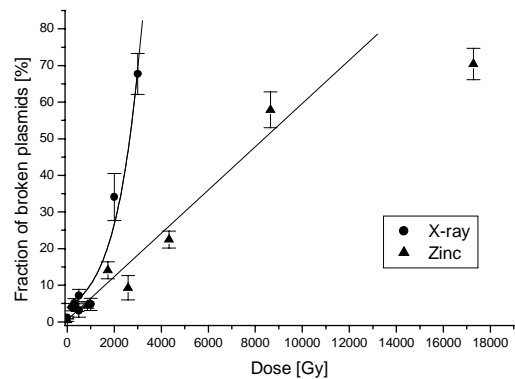


Figure 2: Fraction of broken plasmids

Figure 3 shows that the number of DSB per broken plasmid after high-LET irradiation with low doses is significantly higher than 1. After low doses of X-ray irradiation this number appears to be smaller than that after ion irradiation but it increases steeper with dose.

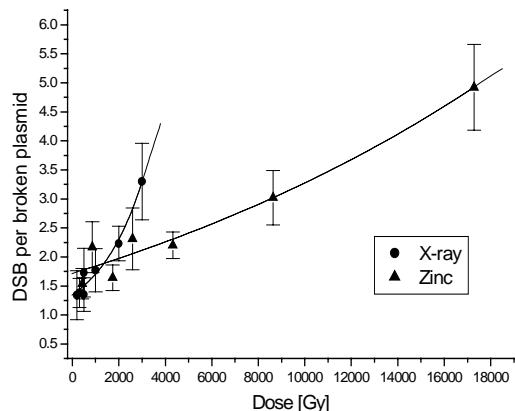


Figure 3: Number of DSB per broken plasmid

These results point to a spatial correlation of the induction of DSB's by densely ionising particles. Yields of DSB per broken plasmid need to be further investigated at low fluences.

[1] W. K. Weyrather et al.; Int. J. Radiat. Biol. 75, 11, 1357-1364 (1999)

[2] G. Taucher-Scholz et al.; Radiat. Environ. Biophys. 34, 101-106 (1995)

Preparation of diode-like single-ion track-etch membrane using combination of chemical and electro-stopping

Apel P.Yu.¹, Korchev Yu.E.², Siwy Z.³, Spohr R.⁴, Yoshida, M.⁵

¹Flerov Laboratory of Nuclear Reactions, JINR, 141980 Dubna, Moscow Region, Russia

²Imperial College London, London W12 0NN, England

³Silesian University of Technology, 44100 Gliwice, Poland

⁴GSI Darmstadt, Planckstr. 1, D-64291 Darmstadt, Germany

⁵JAERI, Takasaki, Watanuki 1233, Takasaki, Gunma-Ken, 37012, Japan

Particle track etching has found diverse uses in science and technology [1]. Production of porous membranes stands out among other applications of the track-etch technique. In the past decade special attention was paid to the study of track-etch nanopores in poly (ethylene terephthalate) (PET) with respect to their ability to mimic biological ion channels (e.g. [2, 3]). Artificial cylindrical channels of few nanometers diameter and 5 or 10 micrometer length exhibited electrical and electro-kinetic properties similar to those observed earlier for biological membranes. One should realize however that the dimensions of artificial nanopores prepared by the track-etch method differ strongly from typical dimensions of biological ion channels e.g. the length of a pore in a PET membrane is app. 10 000 larger than biological channel length. We have aimed therefore at preparing a track-etch pore with dimensions closer to biological ion channels. One way to do that is based on preparation of a strongly asymmetric track-etch whereby the short and narrow part at the tip of the etch pit determines the electric properties of the whole channel.

For this purpose, a single-ion irradiated PET film is inserted into an electrolytic cell (see Fig. 1) and etched from one side in 9 M Na OH while bathing the other side in a mixture of 2M KCl and 2M HCOOH (1:1 by volume), electrically retracting the OH⁻ ions from the tip of the etch pit during pore break-through.

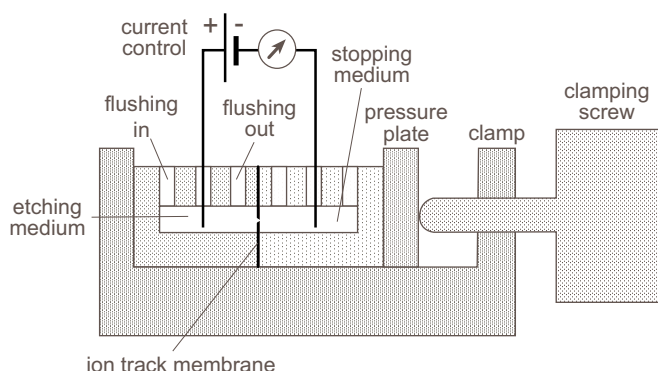


Fig. 1 Cross section of the electrolytic cell used for one-sided etching of ion track membranes. The clamping mechanism ensures a reliable seal ($>10^{12}$ Ohm) between the chamber halves and the membrane.

The process results in the conically shaped pore having wider entrance of app. 800 nm in diameter (measured by SEM)

while the diameter of limiting the transport tip is app. 2 nm (on the basis of PEG permeation). The structure and nature of the tip will be the subject of further investigation.

The electrical properties of the membrane were determined under symmetric bathing conditions of pH and KCl concentration. The current-voltage (I-V) characteristic was measured by stepping the voltage between -5 and $+5$ V. Each measured point corresponds to the current averaged over the dwell time (5 to 10 seconds). An example of observed asymmetric diode-like current-voltage characteristic has been shown in Fig. 2.

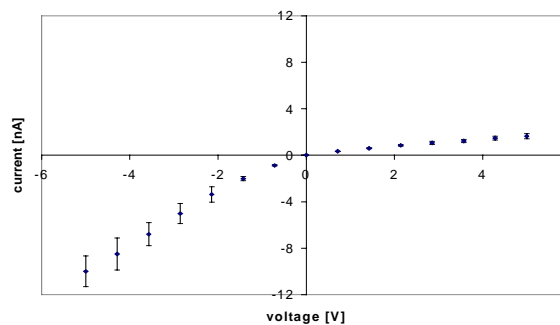


Fig. 2 Intrinsic asymmetry of voltage-gradient stopped single pore membrane. Current – voltage characteristic in symmetric concentration and pH conditions at 0.1 M KCl and pH = 7.

The observed diode-like behavior can be controlled by pH, electrolyte concentration and the pore dimensions. The phenomenon is reproducible and very stable: the same membrane can be studied for many days.

The obtained results have suggested that the one-sided etched pore in a PET membrane can serve as a model of a biological channel. Additionally the diode-like behavior of the membrane enables to use it as an electrical valve.

- [1] Fleischer R.L., Price P.B., and Walker R.M.; Nuclear tracks in solids; Principles and Applications; Univ. of California Press, Berkeley, California, 1975.
- [2] Pasternak C.A., Bashford C.L., Korchev Y.E., Rostovtseva T.K., Lev A.A. *Colloid Surfaces A*, **77** (1993) 119.
- [3] Wolf, A., Siwy, Z., Korchev, Y.,E., Reber, N., Spohr,R. *Cell. Mol. Biol. Lett.* **4** (1999) 553.

Heavy Ion Induced Micropores in Glass as Nucleation Centers of Crystalline Silicon

P.-M. Wilde¹, K. Schmidt¹, P. Schramm¹, J. Vetter², and T. Boeck¹

¹ Institut für Kristallzüchtung im Forschungsverbund Berlin e.V., D-12489 Berlin

² Gesellschaft für Schwerionenforschung mbH, D-64291 Darmstadt

The generation of crystalline structures on amorphous substrates (glass) is of interest in several application fields, as in photovoltaic cells and micro system technique. Glass is useful because it is an electronic insulator, has a high transparency and low thermal conductivity and can be produced in large panes at a low-cost level. However, an epitaxial growth of perfect crystals or crystalline films is not possible due to the lack of lattice structure of this non-crystalline material. A novel method of selective nucleation has been developed to achieve crystalline structures on glass substrate using metallic droplets on the surface acting as nucleation centers [1]. These droplets can be deposited in micropores which are produced by irradiation of the glass samples with heavy ions. At this process ion tracks are created where the network structure of the glass is locally destroyed. We used a borosilicate glass ($T_G < 600^\circ \text{C}$) as substrate material. For irradiation $^{208}\text{Pb}^{n+}$ ($n=28$) ions with energies of 11.4 MeV/nucleon were used applying a dose of $D = 3.3 \cdot 10^5 \text{ ions cm}^{-2}$.

In a subsequent chemical etch treatment of the material the ion traces are enlarged. As etching acid a mixture of HF (40 vol.%), HNO_3 (65 vol.%) and H_2O dest. in a 1:1:1 ratio was used. The etching time of irradiated samples was varied in four steps: 5 s, 20 s, 50 s and 80 s, respectively.

In this way, fields of micropores were generated in the glass surface. Scanning electron microscopy investigations (ZEISS DSM 962) reveal that the pores have a regular conical shape with smooth edges and walls. Depending on the etch time, pore diameters in the range 1,8 - 12 μm can be achieved (fig. 1). The aspect ratio of the pores was found to be 1.4 ± 0.2 (fig. 2). Microdroplets of low melting metals (gallium or indium) were deposited in these cavities by evaporation using the effect of coalescence due to the surface tension of liquid metal (fig. 3). In the next step, evaporated silicon is solved in the metal until droplets are saturated. Under the influence of a temperature gradient, nucleation occurs at the pits of the cavities. Solving additional vaporized silicon in the droplets, the growth of silicon crystallites inside of the cavities is continued. Thus, in each of the pores one silicon crystal is grown which can be observed when the solution is removed (fig. 4). Using this method, glass substrates with areas of more than 15 cm^2 can be covered regularly with silicon crystallites of about 1 μm size and mean distances of 20 μm .

[1] T. Boeck, Th. Teubner, K. Schmidt, P.-M. Wilde: J. Crystal Growth 198/199 (1999) 420-424.

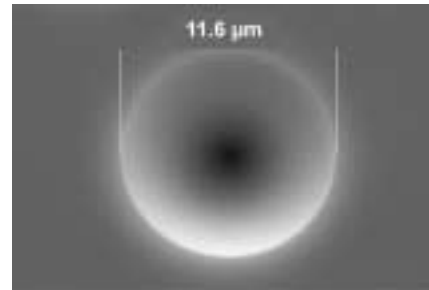


Fig. 1: SEM image of an etched ion track in the glass surface. The pore has a smooth wall and regular edge structure.

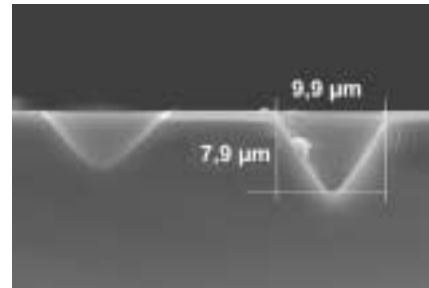


Fig. 2: Cross section of pores in glass with regular cone geometry. The measured aspect ratio is 1.25.

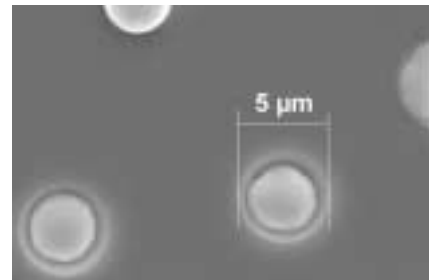


Fig. 3: SEM image of metallic microdroplets which are deposited in the pores.

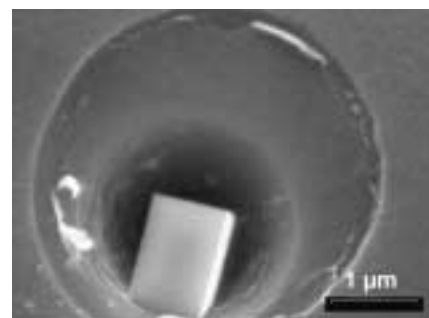


Fig. 4: A silicon single crystal is grown in the microcavity. The circular contour arises from the removed amorphous silicon.

Analysing the electrochemical process of copper deposition in etched ion track membranes

I.U. Schuchert*, D. Dobrev*, M. Martin#, M.E. Toimil Molares*, J. Vetter*
 *GSI, D-Darmstadt, # RWTH Aachen, Inst. Phys. Chem., D-Aachen

Electrochemical techniques are widely used in many different fields. One example is the electrodeposition of copper for the production of printed circuits boards in microelectronics industry [1]. Compared to other methods like chemical and physical vapour deposition, electrochemical techniques have several advantages including avoidance of vacuum systems, high flexibility and low costs. Many investigations are being performed for the creation of novel micro- and nanostructures with high aspect ratios. One method widely used for this purpose is the electrochemical deposition of a metal into the pores of a template, e.g., etched ion track membranes or anodically oxidised aluminium. Nevertheless, up to now very little is known about the mechanism of this process itself [2], for which some similarities to the behaviour of microelectrode ensembles can be expected [3]. Therefore, the potentiostatic electrochemical process of filling etched ion track membranes with copper is studied in detail.

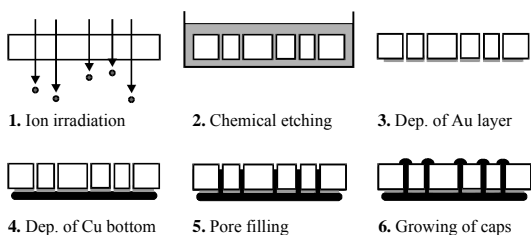


Fig. 1 Template method

Following the template method illustrated in fig. 1 polycarbonate foils with a thickness of 30 μm and a diameter of 5 cm are irradiated at the GSI UNILAC accelerator with Bi ions (11.3 MeV/u) up to a fluence of $1.25 \cdot 10^7$ ions cm^{-2} . Through a chemical etching process the latent ion tracks develop into cylindrical pores with diameters between 400 and 450 nm. A thin gold layer is then sputtered onto one side of the membrane and subsequently reinforced galvanically with copper. This conductive side acts as cathode during pore filling in a specially designed three-electrode cell. A simple salt electrolyte is used containing 2 mol/l H_2SO_4 but only 0.25 mol/l CuSO_4 to neglect mass transport due to migration.

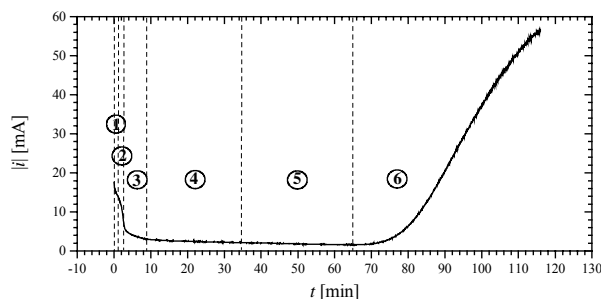


Fig. 2 Current-time-curve for $|\eta| = 120$ mV

In order to analyse the deposition process, current versus time curves are recorded for different applied overvoltages $|\eta|$ (difference between applied and open-circuit potential), namely between 80 and 440 mV. Fig. 2 shows the curve for $|\eta| = 120$ mV. Six different time periods are indicated corresponding to different events determining the overall reaction [4].

As soon as the potential is applied between cathode and reference electrode, copper is deposited and the electrolyte adjacent to the cathode depletes from copper ions – a concentration gradient starts to develop. For very short times (region 1) this gradient is nearly zero so that the charge transfer reaction $\text{Cu}^{2+} + e^- \rightarrow \text{Cu}^+$ determines the deposition process. Within region 2, the transition from charge transfer to diffusion control takes place - both overvoltages are of comparable size. With increasing time the depletion zone in front of the cathode (Nernst layer) is growing into the electrolyte - the concentration gradient is increasing and the over all reaction starts to be diffusion controlled. First, the thickness of the Nernst layer is smaller than the remaining pore length and the diffusion is linear inside the pores (region 3), compare fig. 3A. After some time the depletion zone exceeds the pore length, and a radial diffusion field establishes around each pore (region 4). The ions are diffusing radially towards the pore openings (fig. 3B). For long times (region 5) the radial diffusion fields start to overlap with their neighbours. The diffusion is again linear but now towards the whole membrane surface (fig. 3C). The increase of current in region 6 indicates that caps start to overgrow the membrane surface.

This model describes the deposition process qualitatively and can help to understand the mechanism for different metals in pores with various diameters and aspect ratios. For a quantitative analysis new suitable theories are needed.

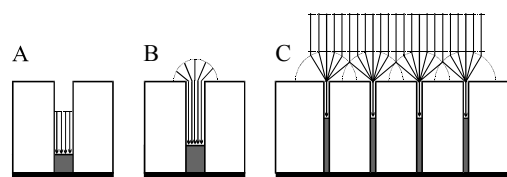


Fig. 3 Diffusion processes during pore filling

References

- [1] J. W. Schultze, V. Tsakova, *Electrochim. Acta* **44** (1999) 3605.
- [2] C. Schönenberger et al., *J. Phys. Chem. B* **101** (1997) 5497.
- [3] K. Aoki, *Electroanalysis* **5** (1993) 627.
- [4] I. U. Schuchert, Doctoral Thesis, TU Darmstadt 2000.

